

Electrochemical Aptamer-Based Biosensors for the Detection of Cardiac Biomarkers

Iwona Grabowska,[†] Neha Sharma,[‡] Alina Vasilescu,[§] Madalina Iancu,^{||} Gabriela Badea,^{||} Rabah Boukherroub,[⊥] Satishchandra Ogale,[‡] and Sabine Szunerits^{*,⊥}

[†]Institute of Animal Reproduction and Food Research, Polish Academy of Sciences, Tuwima 10, 10-748, Olsztyn, Poland

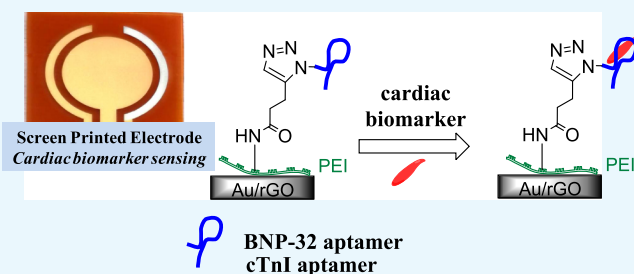
[‡]Indian Institute of Science Education and Research (IISER), 411008, Pune, India

[§]International Centre of Biodynamics, 1B Intrarea Portocalelor, Sector 6, 060101, Bucharest, Romania

^{||}Agrippa Ionescu” Emergency Clinical Hospital, 7 Ion Mincu, 011356, Bucharest, Romania

[⊥]Univ. Lille, CNRS, Centrale Lille, ISEN, Univ. Valenciennes, UMR 8520-IEMN, 59000, Lille, France

ABSTRACT: Rapid and accurate diagnostic technologies for early-state identification of cardiovascular abnormalities have become of high importance to prevent and attenuate their progression. The capability of biosensors to determine an increase in the concentration of cardiovascular protein biomarkers in circulating blood immediately after a myocardial infarction makes them ideal point-of-care platforms and alternative approaches to electrocardiograms, chest X-rays, and different laboratory-based immunoassays. We report here a generic approach toward multianalyte sensing platforms for cardiac biomarkers by developing aptamer-based electrochemical sensors for brain natriuretic peptide (BNP-32) and cardiac troponin I (cTnI). For this, commercial gold-based screen-printed electrodes were modified electrophoretically with polyethyleneimine/reduced graphene oxide films. Covalent grafting of propargylacetic acid integrates propargyl groups onto the electrode to which azide-terminated aptamers can be immobilized using Cu(I)-based “click” chemistry. To ensure low biofouling and high specificity, cardiac sensors were modified with pyrene anchors carrying poly(ethylene glycol) units. In the case of BNP-32, the sensor developed has a linear response from 1 pg mL⁻¹ to 1 μg mL⁻¹ in serum; for cTnI, linearity is observed from 1 pg mL⁻¹ to 10 ng mL⁻¹ as demanded for early-stage diagnosis of heart failure. These electrochemical aptasensors represent a step further toward multianalyte sensing of cardiac biomarkers.



1. INTRODUCTION

The incidence and prevalence of cardiovascular diseases rise in many parts of the world. The need for fast and accurate diagnosis has become crucial to prevent and limit heart failure. Cardiovascular diseases, chronic conditions that get worse over time, are classified into four stages ranging from high risk to advanced heart failure probability, and treatment plans are provided accordingly. It is well known that effective intervention at an early stage can prevent and attenuate their progression. Next to conventional methods for the diagnosis of eventual heart failure, such as electrocardiograms¹ and chest X-rays,² the detection of cardiovascular biomarkers³ provides a simple method for early indication of the disease. The current methods used to identify the presence of cardiac biomarkers are based on antigen–antibody recognition, such as the enzyme-linked immunosorbent assay (ELISA), or rely on fluorescence or radiochemical detection.⁴ Even though these immunoassays are developing rapidly, their main drawbacks are related to long analysis time and cross-reactivity issues. These drawbacks can be overcome by the use of biosensors as cheap and fast detection tools that can be integrated in multiplexed point-of-care devices.⁵ The development of

various sensors for the detection of cardiovascular biomarkers is consequently rapidly advancing,⁶ with electrochemical transduction being one of the most advanced methods in this field for fast and accurate sensing.^{7–11}

We have, for example, shown recently that nitrogen-doped reduced graphene oxide (N-prGO)-modified electrodes when covalently modified with Tro4 aptamers result in electrochemical sensors applicable for cardiac troponin I (cTnI) detection down to 1 pg mL⁻¹.⁷ These sensors specified that acute myocardial infarction (AMI)-diagnosed patients, the most immediately life-threatening syndrome, leading to particularly severe cardiac events, such as irreversible damage in the myocardium, have a saliva cTnI level as high as 675 pg mL⁻¹.

Next to cTnI, B-type natriuretic peptide (BNP) and N-terminal pro-B-type natriuretic peptide (NT-pro-BNP) have been recognized as powerful cardiovascular biomarkers for acute heart failure.¹² These natriuretic peptides are released in

Received: July 6, 2018

Accepted: September 7, 2018

Published: September 26, 2018

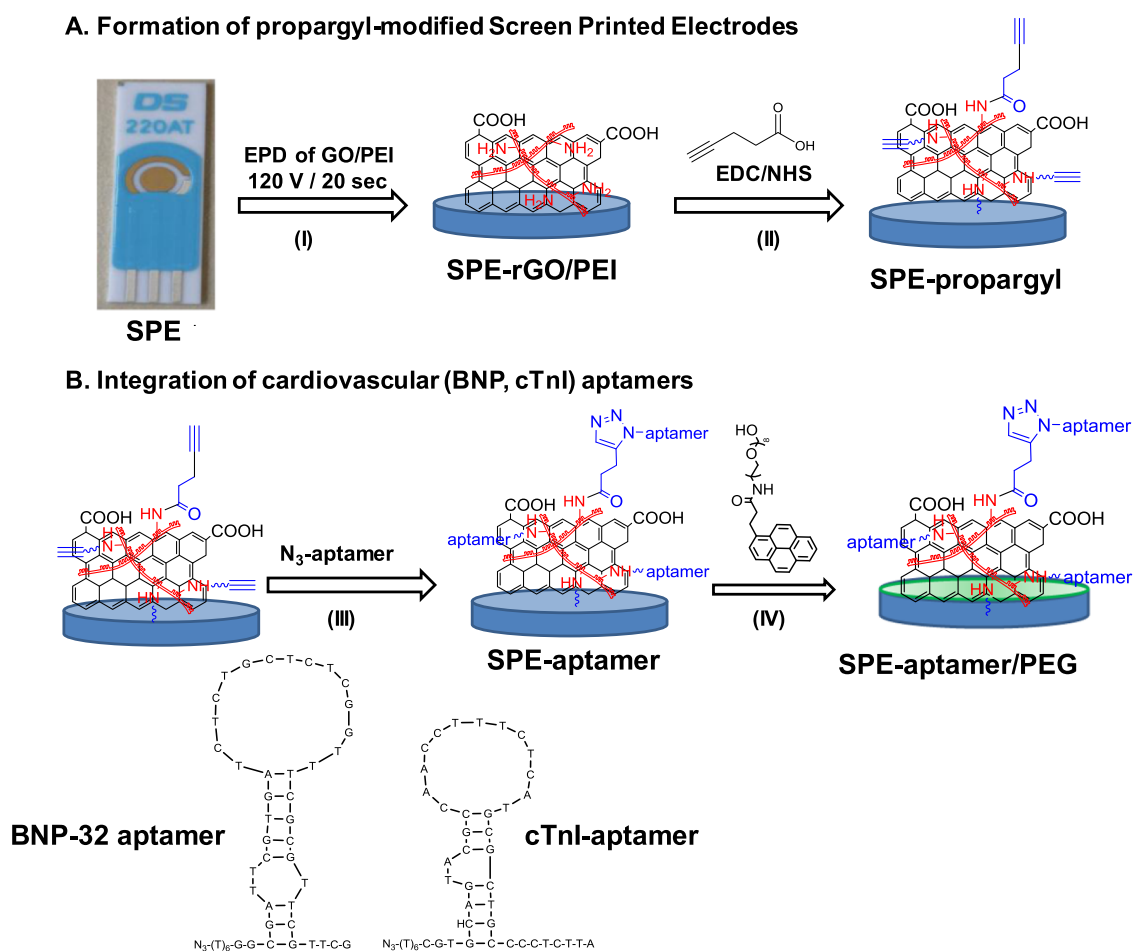


Figure 1. Concept of the construction of electrochemical aptasensor for the sensing of cardiovascular biomarkers BNP and cTnI: (A) formation of the interface: (I) electrophoretic deposition (EPD) of a solution of GO/PEI on gold SPE forming a rGO/PEI thin film and (II) amide bond formation between the acid groups of propargylacetic acid and NH_2 groups of PEI by EDC/NHS chemistry; (B) integration of aptamers (III) using Cu(I)-catalyzed click chemistry to N_3 -modified DNA aptamer and (IV) passivation with synthetic pyrene-PEG (green layer).

response to pressure overload in ventricles and increased stress on ventricular walls. BNP is first synthesized as pre-pro-BNP, which upon proteolytic processing is split into BNP and the amino terminal fragment NT-pro-BNP, with no biological activity. In clinical practice, NT-pro-BNP detection is mostly performed as NT-pro-BNP has a circulation time of about 1–2 h, while that of BNP is only 20 min. Nevertheless, BNP would be the more desirable biomarker for heart failure considering the rapid release and diffusion from the injured tissue to the blood. Moreover, it has a well-defined cutoff level of 100 pg mL^{-1} .¹³ While both natriuretic peptides are produced similarly, plasma levels of NT-proBNP are influenced by renal functions¹⁴ and are strongly susceptible to the age of the patient. However, the detection of BNP is more challenging compared to other cardiovascular biomarkers, as the BNP blood level in healthy patients is low (20 pg mL^{-1} ; 6 pM) and rises to only about 2 ng mL^{-1} (600 pM) in patients with acute heart failure.¹⁵ This might be the reason why there are a limited number of sensors for BNP described so far. A miniaturized immunosensor was reported by Niwa and co-workers and reached a detectable concentration range of 5 pg mL^{-1} to 100 ng mL^{-1} .¹⁶ One of the first electrochemical biosensors for BNP is that of Matsuura et al. with a reported detection limit of $20\text{--}40 \text{ pg mL}^{-1}$, on the limit to detect basal levels of BNP in blood.^{17,18} It relies on acetylcholinesterase-

labeled anti-BNP antibodies undergoing an immunological reaction with BNP. The assay is rather long (2 h) to complete, and the analysis has to be performed in deaerated alkaline solution. An optical lateral flow immunoassay has been recently proposed by Gong et al. using gold nanoparticles modified with BNP antibodies, which reached a detection limit of BNP down to 100 pg mL^{-1} using a simple assay format.¹⁹ Electrical impedance measurements in silicon nanowells have been proposed by Prasad et al. for BNP using anti-BNP as a specific ligand with a detection limit of 1 ag mL^{-1} .²⁰ The group of Pingarron has reported recently the electrochemical detection of BNP down to 4 pg mL^{-1} involving peroxidase-labeled BNP antibodies on screen-printed carbon electrodes modified with gold nanoparticles.⁹ Esteban-Fernández de Ávila et al.²¹ proposed carbon-based screen-printed electrodes (SPE) as ideal interfaces for the simultaneous and independent amperometric detection of NT-pro-BNP and cardiac reactive protein (CRP). Bruno et al. demonstrated the interest of an aptamer–magnetic bead electrochemiluminescence sandwich assay for the detection of BNP with a pg mL^{-1} detection limit.²² The assay used SPE modified with magnetic beads with covalently immobilized NT-proBNP antigen or anti-CRP specific capture antibodies to trap the biomarkers. This was followed by analyte quantification via indirect competitive and sandwich-type immunoassays, respectively, using horseradish

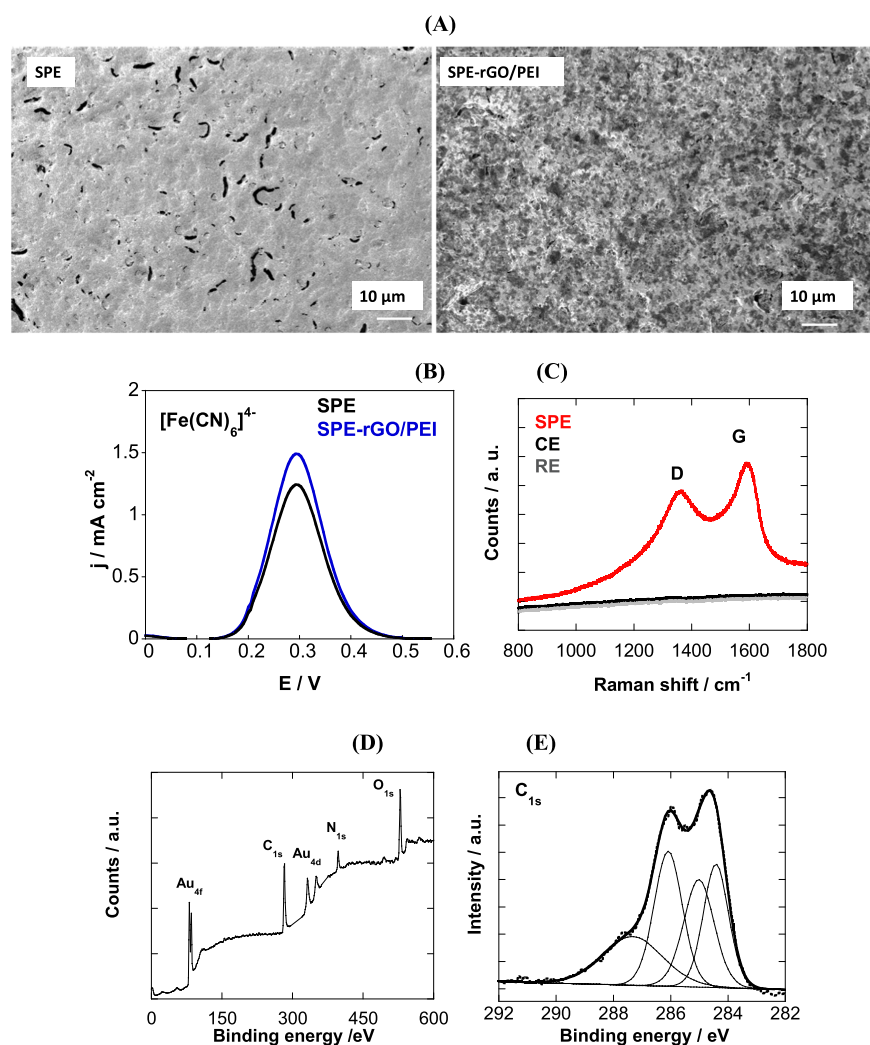


Figure 2. (A) SEM images of SPE before and after electrophoretic coating with rGO/PEI at 120 V_{DC} for 20 s. (B) Differential pulse voltammograms of SPE (black) and SPE-rGO/PEI (blue) recorded in $[\text{Fe}(\text{CN})_6]^{4-}$ (5 mM)/KCl (0.1 M). (C) Raman images recorded at different positions on the electrodes. (D) X-ray photoelectron spectroscopy (XPS) survey spectrum of SPE modified electrophoretically with rGO/PEI. (E) C_{1s} core-level spectrum of SPE-rGO/PEI.

peroxidase-labeled tracers. The developed methodology achieved detection limits of only 470 pg mL^{-1} for both analytes.

We show in this work that commercially available gold-based screen-printed electrodes when modified electrophoretically by a polyethyleneimine (PEI)/reduced graphene oxide (rGO) nanocomposite film result in robust and sensitive electrochemical platforms for the sensing of BNP in serum without the need for any label (Figure 1). Branched PEI was previously proposed as an effective linker for the quantitative immobilization of biomolecules in sensing platforms with electrochemical detection.¹¹ In this work, the presence of NH_2 groups on PEI (Figure 1) allows the covalent linking of BNP-specific ligands, DNA aptamers in our case. Their affinity to specific epitopes on target proteins such as BNP is defined by their sequences, selected *in vitro* by an iterative and stringent process. Unlike antibodies, aptamers have the advantage of being produced in a fast, reproducible manner and in large quantities. Their interest for sensing platforms is in addition related to their increased stability, thus representing stable and innovative ligands for biosensors. Despite their great potential, aptamers are yet to be more widely integrated into biosensors and tested under

clinically relevant conditions. The strategy proposed in this work allows achieving sub-pM BNP detection limits in serum without the need for any amplification strategy. The possibility of sensing using screen-printed electrodes makes this approach, in addition, appropriately operational for parallel multianalyte sensing, which will be exemplified in sensing cardiac troponin I (cTnI) using the same strategy as developed for BNP, by simply changing the used aptamer.

2. RESULTS AND DISCUSSION

2.1. Electrophoretic Modification of Screen-Printed Electrodes.

SPEs were used in this work to bring the sensor as close as possible to practical application. Using integrated systems like this, the question remains how to modify selectively the working electrode over the counter and reference electrodes to maintain good electrochemical performance. Some of us have shown that electrophoretic deposition (EPD) is beneficial for coating sensors as it enables to obtain homogeneous coatings of controlled thickness. More recently, we have shown that EPD can be applied to modify working electrodes in electrochemical microsystems using an optimized process by mixing PEI with GO for cathodic EPD.²³

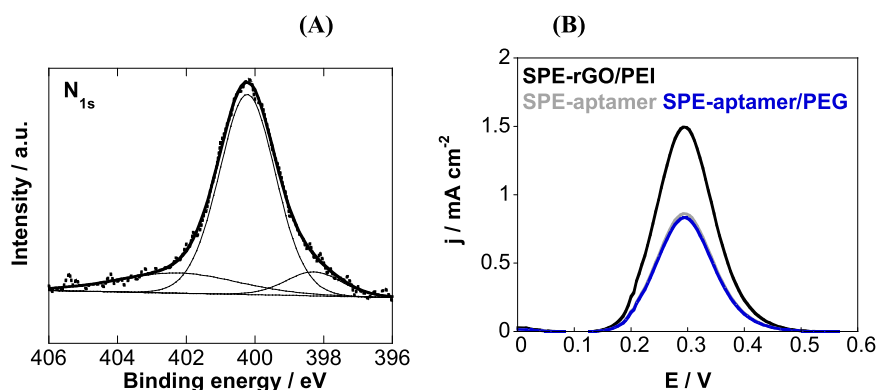


Figure 3. (A) N_{1s} core-level spectrum of SPE-rGO/PEI-aptamer and (B) differential pulse voltammograms of SPE-rGO/PEI (black) SPE-aptamer (gray) and SPE-aptamer/PEG (blue) using $[\text{Fe}(\text{CN})_6]^{4-}$ (5 mM)/PBS (0.1 M).

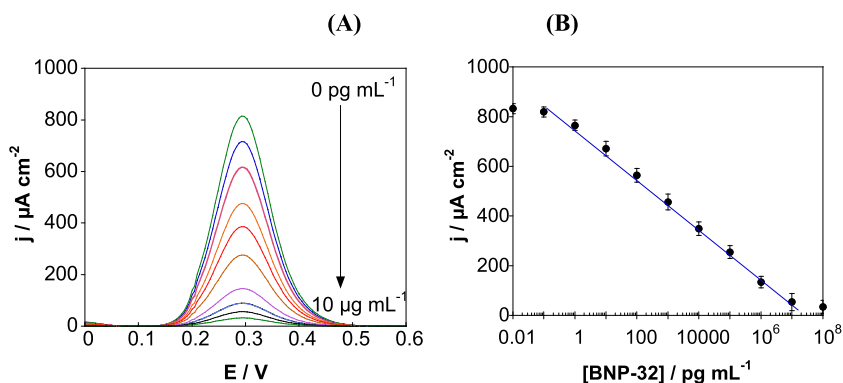


Figure 4. (A) Differential pulse voltammograms at various BNP-32 concentrations (0, 0.01, 0.1, 1, 10, and 100 pg mL^{-1} ; 1, 10, and 100 ng mL^{-1} ; and 1 and 10 $\mu\text{g mL}^{-1}$) recorded with SPE-rGO. (B) Calibration curve for BNP-32 obtained with the aptasensor (error bars refer to the standard deviation for $n = 5$ determinations).

Charging of GO with a cationic polymer such as polyethyleneimine (PEI) results in a positive ζ -potential of $+36.4 \pm 1.3$ mV and well-reduced graphene oxide thin films. Figure 2A shows the scanning electron microscopy (SEM) images of SPE before and after modification with rGO/PEI upon the application of $+120 \text{ V}_{\text{DC}}$ for 20 s. In the case of SPE, cracks in the surface of the electrode are clearly visible. After EPD of rGO/PEI the surface roughness is increased and a homogeneous deposit is observed over the entire surface. These films have a thickness of 3 nm.

Figure 2B exhibits the differential pulse voltammograms of the SPE using $[\text{Fe}(\text{CN})_6]^{4-}$ as the redox probe, before and after coating with rGO/PEI through electrophoretic deposition. The real electrochemically active surface area of the SPE-rGO/PEI electrodes is 0.149 cm^2 as determined by plotting the peak current against the square root of the scan rate,⁷ and is 18% higher than the geometrical area. Taking into account the real electrochemically active area, it becomes evident that coating SPE with a thin rGO/PEI film results in an increase of the anodic peak current. The magnitude of the current correlates with the good electronic properties of the rGO/PEI film, enhanced surface area, and favorable electrostatic interactions between the negatively charged redox probe and the positively charged rGO/PEI interface as reported previously.²⁴ The selective formation of the rGO/PEI film on the gold working electrode is further validated by recording Raman spectra at different parts of the SPE (Figure 2C). The D- and G-bands are located at 1350 and 1582 cm^{-1} , respectively, with an $I_{\text{D}}/I_{\text{G}}$ ratio of 0.89 for rGO/PEI, higher

than that of GO with $I_{\text{D}}/I_{\text{G}} = 0.71$.²⁵ No Raman spectrum was obtained outside the modified gold microelectrode, notably on the reference electrode and on the counter electrode, indicating that the deposition process is highly selective.

The XPS survey spectrum of the rGO/PEI films (Figure 2D) features peaks at binding energies of 285, 532, and 400 eV due to C_{1s} , O_{1s} , and N_{1s} respectively. In addition, bands due to $\text{Au } 4f_{7/2}$ (85 eV), $\text{Au } 4d_{5/2}$ (335 eV), and $\text{Au } 4d_{3/2}$ (333 eV) are observed, indicating that the rGO/PEI layer is below 10 nm. The amount of N_{1s} is determined to be 9.5 atom %. The C_{1s} core-level XPS image of SPE-rGO/PEI (Figure 2E) displays the characteristic bands of rGO at 284.4 eV (sp^2 -hybridized carbon), together with bands at 285.0 eV (sp^3 -hybridized carbon/C–H), 286.1 eV (C–O/C–N), and 287.2 eV (C–OX).²⁶

2.2. Functionalization of SPE-rGO/PEI Electrodes. The integration of propargyl functions onto SPE-rGO/PEI was achieved through covalent linking of propargylacetic acid (Figure 1) to the NH_2 groups of PEI using classical EDC/NHS chemistry. The SPE-propargyl electrode can be further modified via click chemistry with aptamer ligands (Figure 1).^{27,28} The BNP aptamer chosen was aptamer A10 (Figure 1) as proposed by Wang et al. by the SELEX process selection.²⁹ This aptamer is reported to have a dissociation constant of $K_{\text{d}} = 12 \pm 0.1 \text{ nM}$ for BNP-32 peptide and be highly selective.²⁹ In the case of cardiac troponin I protein sensing, we used the Tro4 aptamer with a reported $K_{\text{d}} = 270 \text{ pM}$,³⁰ and it was shown to be adequate for the formation of a selective electrochemical aptasensor for cTnI.⁷

Table 1. Characteristics of Electrochemical BNP Sensing Platforms^a

method	interface	LOD (pg mL ⁻¹)	linear range (ng mL ⁻¹)	ref
LSV	immune reaction in solution using AChE-labeled anti-BNP antibodies, detection on silver electrodes by measuring unreacted conjugates from enzymatic reaction	20 000	20–100	17
LSV	immune reaction in solution with BNP-modified Au NPS detection on a silver electrode modified with thiocholine	20	0.02–0.2	18
SPR	gold modified with cystamine and BNP and anti-BNP-AChE conjugate	5	0.005–100	16
CV	SPE modified with Au NPs/BNP antibody and HRP-antibody (sandwich assay)	4	0.014–15	9
DPV	SPE-aptamer/PEG	0.9	0.0009–1000	this work
EIS	silicon nanowells modified with anti-BNP	0.001	0.000001–10 000 (DR)	20

^aAu NPs, gold nanoparticles; AChE, acetylcholine esterase-labeled antibody; LSV, linear sweep voltammetry; DR, dynamic range.

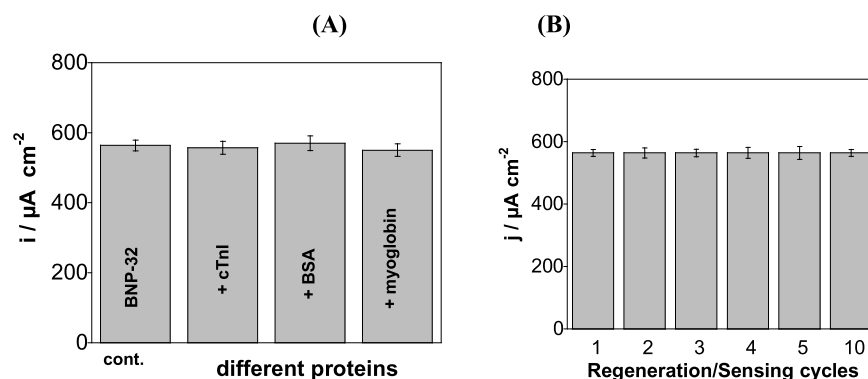


Figure 5. (A) Specificity of the SPE-aptamer/PEG sensors determined in $[\text{Fe}(\text{CN})_6]^{4-}$ (5 mM)/PBS (0.1 M) in BNP-32 (100 pg mL^{-1}) being the control (cont.) in the presence of cTnI (6 $\mu\text{g mL}^{-1}$), BSA (60 mg mL^{-1}), and myoglobin (1.0 mg mL^{-1}) and (B) reusability after immersion into NaOH (0.1 M, pH 12.0) for 20 min. The signal recorded for a concentration of BNP-32 peptide of 100 pg mL^{-1} was taken as the reference (error bars refer to the standard deviation for $n = 5$ determinations).

The effectiveness of the surface modification procedure used was confirmed by the high-resolution N_{1s} XPS image (Figure 3A). It reveals a band at 400.2 eV due to the nitrogen in the triazole ring ($\text{N}=\text{N}-\text{N}$) and amide bonds ($\text{NH}-\text{C}=\text{O}$) as well as a band at 402.4 eV ($\text{N}=\text{N}-\text{N}$) with an additional band at 398.2 eV due to the nitrogen in PEI.

The electrochemical behavior of the SPE-aptamer electrode using $[\text{Fe}(\text{CN})_6]^{4-/3-}$ as a redox couple is seen in Figure 3B. Integration of the aptamer results in decreased current due to the incorporation of aptamers carrying negatively charged phosphate backbones. Further immersion into pyrene-PEG, where the lipophilic pyrene part adheres strongly to rGO/PEI and the PEG unit confers the surface with antifouling properties, does not affect strongly the charge transfer.²⁴

3.3. Electrochemical Sensing of BNP-32 Peptide. Differential pulse voltammetry (DPV) using $[\text{Fe}(\text{CN})_6]^{4-}$ as a redox probe was used for the detection of BNP-32 peptide with the developed aptasensor. Addition of BNP-32 results in a decrease of the redox current (Figure 4A) as the complex formed between the aptamer and the peptide acts as a diffusion barrier, hindering the charge transfer from the redox probe $[\text{Fe}(\text{CN})_6]^{4-}$ to the electrode surface. The sensor exhibits excellent analytical performance for BNP-32 detection (Figure 4B) with a wide linear range between 1 pg mL^{-1} and 1 $\mu\text{g mL}^{-1}$ and correlation of j ($\mu\text{A cm}^{-2}$) = $771.2 - 105.2 \log[\text{BNP} - 32]$ (pg mL^{-1}) ($R^2 = 0.9992$). From a signal/noise ratio of 3/1 using intra-day assays, a detection limit of about 0.9 pg mL^{-1} is determined. As the blood BNP level under normal conditions is about 20 pg mL^{-1} , the detection limit is appropriate for analyzing blood samples with the aptasensor. Moreover, acute heart failure rises BNP concentration to levels

around 2 ng mL^{-1} , where the sensor is still in its linear range.¹⁵ This sensor format was also competitive with other reported BNP sensing schemes (Table 1) in terms of not only sensitivity but also simplicity, as it did not require the use of any enzyme or nanoparticle amplification.

The sensor proved to be specific for BNP-32 (Figure 5A). A significant decrease of the current density is observed in the presence of 100 pg mL^{-1} BNP-32, while addition of several times higher concentrations of cTnI (6 $\mu\text{g mL}^{-1}$), myoglobin (1.0 mg mL^{-1}), or bovine serum albumin (BSA) (60 mg mL^{-1}) did not alter the electrochemical signal.

Moreover, the reproducibility of the aptasensor fabrication was evaluated by testing its performance for BNP-32 sensing on different electrodes (intra-day assays) and the coefficient of variation of the signal recorded for 100 pg mL^{-1} BNP-32 was 5.9% for $n = 10$ electrodes. When stored at 4 °C in PBS for 1 month, the aptasensor response for 100 pg mL^{-1} BNP-32 decreased by 4%, indicating good storage stability.

While disposable sensors are relevant for endpoint measurements in clinical settings (e.g., to minimize the risk of contamination), reusable devices are desirable for studies monitoring the biomarker–drug interaction or the evolution of cardiac biomarkers levels in a patient. With progress in automation and miniaturization, sensor reusability remains an important feature. By immersing the BNP-32 aptasensor into NaOH (0.1 M, pH 12.0) for 20 min, the aptamer/BNP bond was broken and the aptamer-based sensor coating was regenerated, enabling sensor reuse. As demonstrated in Figure 5B, this cleaning and surface regeneration procedure does not affect the sensitivity of the measurements for up to 10 tested regeneration/sensing cycles.

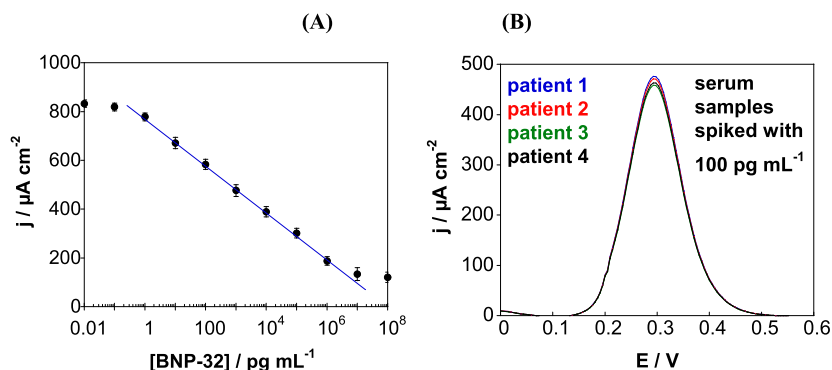


Figure 6. (A) Change in current density determined by DPVs in human serum spiked with various BNP-32 concentrations. (B) DPV response of serum samples of four different patients spiked with 100 pg mL⁻¹ BNP-32 (results represent the average of $n = 3$ determinations).

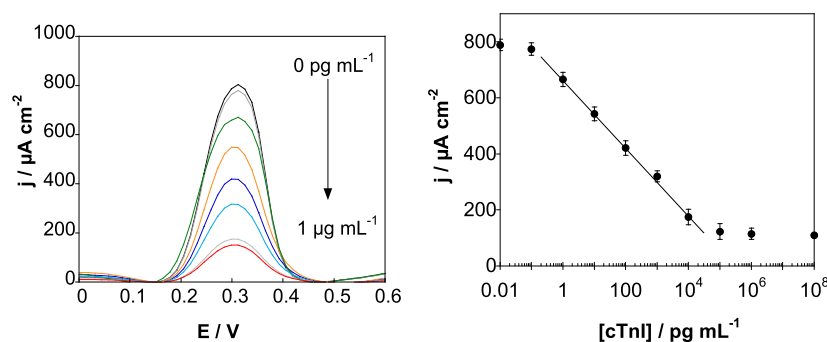


Figure 7. (A) DPV at various cTnI concentrations recorded with an SPE-aptamer/PEI sensor. (B) Calibration curve for cTnI obtained with the aptasensor (error bars refer to the standard deviation for $n = 5$ determinations).

The novel sensor was furthermore tested in biological fluids. For this purpose, we spiked human serum samples with BNP-32 standards (Figure 6). From the calibration curve (Figure 6A), a linear relationship between current density and BNP-32 concentration between 1 pg mL⁻¹ and 1 μg mL⁻¹ is seen according to j (μA cm⁻²) = 773.9 - 96.5 log[BNP - 32] (pg mL⁻¹)... ($R^2 = 0.9995$). In comparison to the calibration curve obtained in PBS (Figure 4B), the sensitivity and the linear range are somehow reduced. The limit of detection was estimated to be 1 pg mL⁻¹, comparable to the sensors in PBS.

2.4. Sensing of cTnI in Serum Samples. To validate if the proposed sensor strategy can be used for other aptamers, a different SPE-propargyl electrode was modified via click chemistry with cardiac troponin I (cTnI), an aptamer ligand with a reported $K_d = 270$ pM.³⁰ Using DPV and [Fe(CN)₆]⁴⁻, a linear range between 1 pg mL⁻¹ and 10 ng mL⁻¹, a correlation of j (μA cm⁻²) = 666 - 121 log[cTnI] (pg mL⁻¹)... ($R^2 = 0.9992$), and a detection limit of 1 pg mL⁻¹ are determined (Figure 7). The sensing characteristics are in line with real demands with the cutoff level for cTnI in serum for acute coronary syndrome (ACS) being 50 pg mL⁻¹.

2.5. Sensing in Real Samples for Clinical Diagnosis. Finally, serum samples, obtained from patients who reported heart failure symptoms, were analyzed. Patient 1 showed a cTnI level of 3 pg mL⁻¹, comparable to the classical enzyme-linked fluorescence assay (ELFA) test (Table 2). This level in addition ruled out any ACS. Increased cTnI levels were found for the other patients.

In the case of BNP-32, in all of the samples, no BNP-32 could be detected. This was confirmed by using the i-STAT BNP test (Abbott), a two-site enzyme-linked immunosorbent assay, with a detection limit of 15 pg mL⁻¹.³¹ However, NT-

Table 2. BNP-32 Concentrations in Serum of Four Different Patients with Reported Heart Failure Symptoms Determined by the Electrochemical Aptasensor and by a Hospital's Laboratory Assay^a

serum sample	aptasensor for BNP-32 (pg mL ⁻¹)	ELISA for BNP-32 (pg mL ⁻¹)	ELFA for NT-proBNP (pg mL ⁻¹)	aptasensor for cTnI (pg mL ⁻¹)	ELFA for cTnI (pg mL ⁻¹)
1	—	*	30	3 ± 1	2.9
2	—	*	1140	40 ± 5	43
3	—	*	10 931	125 ± 10	118
4	—	*	17 680	189 ± 15	178
analysis of serum samples spiked with 100 pg mL ⁻¹ BNP-32 with the aptasensor					
sample	BNP-32, pg mL ⁻¹		recovery (%)		
1 (spiked)	98 ± 2		98		
2 (spiked)	102 ± 2		102		
3 (spiked)	106 ± 4		106		
4 (spiked)	108 ± 2		108		

^aAverage of $n = 3$ assays.

proBNP could be detected in these samples using the ELFA. This is in line with the fast degradation of BNP-32 to NT-proBNP. Normal concentrations of NT-proBNP are 10–300 pg mL⁻¹, which indicates that patients 2–4 are high-risk individuals for major cardiovascular events. These results also validate that there is no direct correlation between BNP-32 and NT-proBNP levels in blood.^{32,33}

To check the accuracy of the electrochemical aptasensor for higher BNP-32 concentrations, the serum samples of all four patients were spiked with 100 pg mL⁻¹ BNP-32, the cutoff level for positive ACS diagnosis. From the current response

(Figure 6B), total BNP-32 concentrations between 98 and 108 pg mL⁻¹ could be determined with a coefficient of variation for the various samples between 1.85 and 3.77% ($n = 3$ assays). The 98–108% recovery, correlated with excellent repeatability indicates the very good accuracy of the BNP aptasensor.

3. CONCLUSIONS

A robust and sensitive electrochemical aptamer-based sensor for the sensitive detection of two cardiovascular biomarkers, BNP and cTnI, was obtained starting from commercially available gold-based screen-printed electrodes that were coated by EPD with a PEI/rGO nanocomposite film. The presence of the NH₂ groups in PEI facilitated the linking of a BNP-32 and cTnI aptamer via grafting a propargylacetic acid linker followed by Cu(I)-based click-chemistry attachment of the azide-terminated aptamer. While the use of specific aptamers with dissociation constants in pM and nM ranges (for cTnI and BNP-32, respectively) ensured highly sensitive recognition of the targeted biomarkers even in complex matrices such as serum, the presence of rGO in the nanocomposite coating enabled facile protection against nonspecific interactions with other proteins, simply by immersion into poly(ethylene glycol)-modified pyrene. The sensor design leads to a sensitive electrochemical platform for the detection of BNP in serum without the need for any label with a limit of detection of 0.9 pg mL⁻¹ and high accuracy demonstrated based on measurements of serum samples spiked with BNP-32. Moreover, reuse of more than 10 assays without significant loss in sensitivity was demonstrated.

To prove that the approach is generic and can be extended to other aptamers to advance toward multianalyte platforms for cardiac biomarker detection, we have applied the same procedure for the cardiac troponin aptamer. Serum samples from patients suspected of ACS were analyzed in parallel with the aptasensors for BNP-32 and cTnI and by the standard kits used in the hospitals, and a good agreement was determined. The proposed reusable electrochemical aptasensors for BNP-32 and cTnI, based on screen-printed electrodes, represent an advance toward cost-effective multianalyte platforms for cardiac biomarker detection. Indeed, a thorough diagnosis and monitoring of people with cardiac conditions is in line with the current trend for multiplexed point-of-care devices, as it requires simultaneous detection of multiple parameters, including, besides BNP-32 and cTnI, biomarkers such as N-terminal proBNP (NT-proBNP) and C reactive protein (CRP). The approach demonstrated here will be advanced toward complete, “hybrid” systems for cardiac monitoring, including not only aptamers but also antibodies or peptides as biorecognition elements for best specificity and sensitive detection of cardiac biomarkers. Integration with screen-printed eight-electrode arrays is the next step in this direction as it will allow parallel testing of a higher number of samples in clinical laboratories for the validation of the proposed devices.

4. EXPERIMENTAL SECTION

4.1. Materials. Potassium hexacyanoferrate(II) ([K₄Fe(CN)₆]), hydrazine hydrate, triethylamine ($\geq 99.5\%$, TEA), *N,N'*-disuccinimidyl carbonate ($\geq 95.0\%$, DSC), dichloromethane ($\geq 99.8\%$, CH₂Cl₂), phosphate buffer tablets (PBS, 0.1 M), *N*-(3-dimethylaminopropyl)-*N'*-ethylcarbodiimide hydrochloride (EDC), *N*-hydroxysuccinimide (NHS), propargylacetic acid, copper(II) sulfate pentahydrate, sodium

ascorbate, tris(3-hydroxypropyltriazolylmethyl)amine (THPTA), polyethyleneimine (branched PEI), BSA, and myoglobin were provided by Sigma-Aldrich. Graphene oxide (GO) powder was obtained from Graphenea, Spain.

PEGylated pyrene units were synthesized as reported earlier by our group.²⁴

The 5'-azide-modified 40-base DNA BNP aptamer (with the sequence 5'-N₃-TTT-TTT-GGC GAT TCG TGA TCT CTG CTC TCG GTT TCG CGT TCG TTC G-3')²⁹ and the cardiac troponin I aptamer (with the sequence 5'-N₃-TTT-TTT-CGT GCA GTA CGC CAA CCT TTC TCA TGC GCT GCC CCT)³⁰ were provided by Integrated DNA Technologies (Leuven, Belgium).

BNP-32 peptide (MW = 3.4 kDa) was obtained from BACHEM AG (Switzerland). Human cardiac troponin I protein (MW = 24 kDa) was obtained from Abcam (Cambridge, UK).

The enzyme-linked fluorescence assay (ELFA) MiniVidas NT-proBNP kit and Vidas Troponin kits were obtained from bioMérieux. The i-STAT BNP test (Abbott), a two-site enzyme-linked immunosorbent assay, was used for the quantitative measurement of BNP-32.³¹

Screen-printed electrodes (SPE) with a gold working electrode ($A = 0.125 \text{ cm}^2$), a gold auxiliary electrode, and a Ag reference electrode were obtained from DropSens, Spain.

Serum samples were collected from a peripheral vein of patients admitted under suspicion of heart failure in the Cardiology Department of “Agrippa Ionescu” Emergency Clinical Hospital, Bucharest, Romania. The studied samples were provided as per the medical protocol for heart failure suspicion and stored at $-70 \text{ }^\circ\text{C}$. The study was approved by the Hospital's Ethics Committee, and all of the patients signed an informed consent.

4.2. Electrophoretic Deposition of rGO/PEI. GO/PEI dispersions were obtained by mixing GO (1 mg mL⁻¹) and PEI (1 mg mL⁻¹) for 48 h at room temperature under stirring. Gold-based SPEs were coated with a thin layer of PEI/rGO by a cathodic electrophoretic deposition process by applying a direct current voltage of 120 V for 20 s between the SPE (cathode) and a Pt plate (anode).

4.3. Formation of Aptamer Sensors (SPE-Aptamer/PEG). Azide-terminated cardiovascular aptamers were “clicked” to SPE-rGO/PEI electrodes by first immersing into EDC (25 mM)/NHS (25 mM) containing propargylacetic acid (20 mM) for 2 h, followed by interaction of 5'-N₃-modified aptamer (1 μM in the presence of 10 mM CuSO₄, 100 mM sodium ascorbate, and 20 mM THPTA) ions for 7 h at room temperature and washing (three times) with PBS. Finally, the electrode was immersed into pyrene-PEG (1 mM)²⁴ for 2 h at room temperature to block nonspecific adsorption. The formed SPE-aptamer/PEG sensors were stored in 0.01 M PBS at 4 $^\circ\text{C}$ before use.

4.4. Electrochemical Sensing. Electrochemical measurements were performed with a potentiostat/galvanostat (Metrohm Autolab, The Netherlands). For the detection of BNP-32 peptide and cTnI protein, differential pulse voltammograms (DPVs) were recorded in a [Fe(CN)₆]⁴⁻ (5 mM) solution in 0.01 M PBS (pH 7.4) under a modulation amplitude of 50 mV with a step potential of 5 mV, a modulation time of 0.05 s, and an interval time of 0.5 s. The SPE-aptamer/PEG electrode was immersed in BNP-32 or cTnI standard solutions or undiluted serum solutions spiked with BNP-32 or cTnI for 30 min. After rinsing with PBS (0.01

M, pH 7.4, three times), the electrodes were immersed in $[\text{Fe}(\text{CN})_6]^{4-}$ (5 mM in 0.1 M PBS, pH 7.4) and a DPV signal was recorded. The aptasensor interface was regenerated upon immersion in NaOH (0.1 M, pH 12.0) for 20 min.

4.5. Surface Characterization. Scanning electron microscopy (SEM) images were obtained using an ULTRA 55 electron microscope (Zeiss, France).

X-ray photoelectron spectroscopy (XPS) was carried out on a PHI 5000 VersaProbe-Scanning ESCA Microprobe (ULVAC-PHI, Japan/USA) instrument at a base pressure below 5×10^{-9} mbar with 90° between the X-ray source. The spectra were decomposed into their components with mixed Gaussian–Lorentzian (30:70) shape lines using CasaXPS software.

ζ -Potential measurements were carried out with a Zeta-sizer Nano-ZS (Malvern Instruments Inc. Worcestershire, UK) at a sample concentration of $10 \mu\text{g mL}^{-1}$ and measured in Milli-Q water at pH 7.0.

AUTHOR INFORMATION

Corresponding Author

*E-mail: Sabine.szunerits@univ-lille.fr.

ORCID

Rabah Boukherroub: 0000-0002-9795-9888

Satishchandra Ogale: 0000-0001-5593-9339

Sabine Szunerits: 0000-0002-1567-4943

Notes

The authors declare no competing financial interest.

ACKNOWLEDGMENTS

Financial supports from the University of Lille, the Centre National de la Recherche Scientifique (CNRS), the Hauts-de-France region, and the Agence Nationale de la Recherche (ANR) through FLAG-ERA JTC 2015-Graphitivity project are acknowledged. I.G. acknowledges support from the KNOW Consortium “Healthy Animal - Safe Food”, MS&HE Decision No. 05-1/KNOW2/2015. S.O. acknowledges the Raman-Charpak fellowship 2017.

REFERENCES

- (1) Scirica, B. M. Acute Coronary Syndrome: Emerging Tools for Diagnosis and Risk Assessment. *J. Am. Coll. Cardiol.* **2010**, *55*, 1403–1415.
- (2) Morales, M.-A.; Prediletto, R.; Rossi, G. G.; Catapano, G.; Lombardi, M.; Rovai, D. Routine Chest X-ray: Still Valuable for the Assessment of Left Ventricular Size and Function in the Era of Super Machines? *J. Clin. Imaging Sci.* **2012**, *2*, 25.
- (3) King, K.; Grazette, L. P.; Paltoo, D. N.; McDevitt, J. T.; Sia, S. K.; Barrett, P. M.; Apple, F. S.; Gurbel, P. A.; Weissleder, R.; Leeds, H.; Iturriaga, E. J.; Rao, A.; Adhikari, B.; Desvigne-Nickens, P.; Galis, Z. S.; Libby, P. Point-of-Care Technologies for Precision Cardiovascular Care and Clinical Research. *JACC Basic Transl. Sci.* **2016**, *1*, 73–86.
- (4) Han, X.; Li, S.; Peng, Z.; Othman, A. M.; Leblanc, R. Recent Development of Cardiac Troponin I detection. *ACS Sens.* **2016**, *1*, 106–114.
- (5) Dincer, C.; Bruch, R.; Kling, A.; Dittrich, P. S.; Urban, G. A. Multiplexed Point-of-Care Testing. *Trends Biotechnol.* **2017**, *35*, 728–742.
- (6) Altintas, Z.; Fakanya, S. M.; Tothill, I. E. Cardiovascular disease detection using bio-sensing techniques. *Talanta* **2014**, *128*, 177–186.
- (7) Chekin, F.; Vasilescu, A.; Jijie, R.; Singh, S. K.; Kurungot, S.; Iancu, M.; Bade, G.; Boukherroub, R.; Szunerits, S. Sensitive electrochemical detection of cardiac troponin I in serum and saliva by nitrogen-doped porous reduced graphene oxide electrode. *Sens. Actuators, B* **2018**, *262*, 180–187.
- (8) Rezaei, B.; Ghani, M.; Shoushtari, A. M.; Rabiee, M. Electrochemical biosensors based on nanofibers for cardio biomarker detection: A comprehensive review. *Biosens. Bioelectron.* **2016**, *78*, 513–523.
- (9) Serafin, V.; Torrente-Rodriguez, R. M.; Gonzalez-Cortes, A.; Garcia de Frutos, P.; Sabaté, M.; Campuzano, S.; Yanez-Sadeno, P.; Pingarron, J. M. An electrochemical immunosensor for brain natriuretic peptide prepared with screen-printed carbon electrodes nanostructured with gold nanoparticles grafted through aryl diazonium salt chemistry. *Talanta* **2018**, *179*, 131–138.
- (10) Shin, S. R.; Zhang, Y. S.; JKim, D.-J.; Manbohi, A.; Avci, H.; Silvestri, A.; Alemna, J.; Hu, N.; Kilic, T.; Keung, W.; Righi, M.; Assawes, P.; Alhadrami, H. A.; Li, R. A.; Dokmeci, M. R.; HKhademhosseini, A. Aptamer-based microfluidic electrochemical biosensors for monitoring cell-secreted trace cardiac biomarkers. *Anal. Chem.* **2016**, *88*, 10019–10027.
- (11) Horak, J.; Dincer, C.; Qelibari, E.; Bakirci, H.; Urban, G. Polymer-modified microfluidic immunochip for enhanced electrochemical detection of troponin I. *Sens. Actuators B* **2015**, *209*, 478–485.
- (12) Maalouf, R.; Bailey, S. A review on B-type natriuretic peptide monitoring: assays and biosensors. *Heart Failure Rev.* **2016**, *21*, 567–578.
- (13) McDonnell, B.; Hearty, S.; Leonard, P.; O’Kennedy, R. Cardiac biomarkers and the case for point-of-care testing. *Clin. Biochem.* **2009**, *42*, 549–561.
- (14) Horii, M.; Matsumoto, T.; Uemura, S.; Sugawara, Y.; Takitsume, A.; Ueda, T.; Nakagawa, H.; Nishida, T.; Soeda, T.; Okayama, S.; Somekawa, S.; Ishigami, K.; Takeda, Y.; Kawata, H.; Kawakami, R.; Saito, Y. Prognostic value of B-type natriuretic peptide and its amino-terminal proBNP fragment for cardiovascular events with stratification by renal function. *J. Cardiol.* **2013**, *61*, 410–416.
- (15) Palazzuoli, A.; Gallotta, M.; Quatrini, I.; Nuti, R. Natriuretic peptides (BNP and NT-proBNP): measurement and relevance in heart failure. *Vasc. Health Risk Manag.* **2010**, *6*, 411–418.
- (16) Kurita, R.; Yokota, Y.; Sato, Y.; Mizutani, F.; Niwa, O. On-chip enzyme immunoassay of a cardiac marker using a microfluidic device combined with a portable surface plasmon resonance system. *Anal. Chem.* **2006**, *78*, 5525–5531.
- (17) Matsuura, H.; Sato, Y.; Niwa, O.; Mizutani, F. Electrochemical Enzyme Immunoassay for a peptide hormone in picomolar levels. *Anal. Chem.* **2005**, *77*, 4235–4240.
- (18) Matsuura, H.; Sato, Y.; Niwa, O.; Mizutani, F. Surface electrochemical enzyme immunoassay for the highly sensitive measurement of B-type natriuretic peptide. *Sens. Actuators, B* **2005**, *108*, 603–607.
- (19) Gong, Y.; Hu, J.; Choi, J. R.; You, M.; Zheng, Y.; Xu, B.; Wen, T.; Xu, F. Improved LFIA for highly sensitive detection of BNP at point-of-care. *In. J. Nanomed.* **2017**, *12*, 4455–4466.
- (20) Prasad, S.; Selvam, A. P.; Reddy, R. K.; Love, A. Silicon nanosensor for diagnosis of cardiovascular proteomic markers. *J. Lab. Autom.* **2013**, *18*, 143–151.
- (21) de Avila, B. E.-F.; Escamilla-Gómez, V.; Lanzone, V.; Campuzano, S.; Pedrero, M.; Compagnone, D.; Pingarrón, J. M. Multiplexed determination of amino-terminal pro-B type natriuretic peptide and C-reactive protein cardiac biomarkers in human serum at a disposable electrochemical magnetoimmunosensor. *Electroanalysis* **2014**, *26*, 254–261.
- (22) Bruno, J. G.; Richarte, A. M.; Phillips, T. Preliminary development of a DNA aptamer-magnetic based capture electrochemiluminescence sandwich assay for brain natriuretic peptide. *Microchem. J.* **2014**, *115*, 32–38.
- (23) Kahlouche, K.; Jijie, R.; Hosu, I.; Barras, A.; Gharbi, T.; Yahiaoui, R.; Herlem, G.; Szunerits, S.; Boukherroub, R. Controlled modification of electrochemical microsystems with polyethylenimine/reduced graphene oxide using electrophoretic deposition: Sensing of dopamine levels in meat samples. *Talanta* **2018**, *178*, 432–440.

(24) Jijie, R.; Kahlouche, K.; Barras, A.; Yamakawa, N.; Bouckaert, J.; Gharbi, T.; Szunerits, S.; Boukherroub, R. Reduced graphene oxide/polyethylenimine based immunosensor for the selective and sensitive electrochemical detection of uropathogenic *Escherichia coli*. *Sens. Actuators B* **2018**, *260*, 255–263.

(25) Subramanian, P.; Niedziolka-Jonsson, J.; Lesniewski, A.; Wang, Q.; Li, M.; Boukherroub, R.; Szunerits, S. Preparation of Reduced Graphene Oxide-Ni(OH)₂ Composites by Electrophoretic Deposition: Application for Non-Enzymatic Glucose Sensing. *J. Mater. Chem. A* **2014**, *2*, 5525–5533.

(26) Dave, K.; Park, K. H.; Dhayal, M. Two-step Process for Programmable Removal of Oxygen Functionality of Graphene Oxide: Functional, Structural and Electrical Characteristics. *RSC Adv.* **2015**, *5*, 95657–95665.

(27) Wang, Q.; Vasilescu, A.; Wang, Q.; Coffinier, Y.; Li, M.; Boukherroub, R.; Szunerits, S. Electrophoretic approach for the simultaneous deposition and functionalization of reduced graphene oxide nanosheets with diazonium compounds: application for lysozyme sensing in serum. *ACS Appl. Mater. Interfaces* **2017**, *9*, 12823–12831.

(28) Xie, D.; Li, C.; Shanguan, L.; Qi, H.; Xue, D.; Gao, Q.; Zhang, C. Click Chemistry-Assisted Self-Assembly of DNA Aptamer on Gold Nanoparticles-Modified Screen-Printed Carbon Electrodes for Label-Free Electrochemical Aptasensor. *Sens. Actuators B* **2014**, *192*, 558–564.

(29) Wang, Y.; Wu, J.; Chen, Y.; Xue, F.; Teng, J.; Cao, J.; Lu, C.; Chen, W. Magnetic microparticle-based SELEX process for the identification of highly specific aptamers for heart marker-brain natriuretic peptide. *Microchim. Acta* **2015**, *182*, 331–339.

(30) Jo, H.; Gu, H.; Jeon, W.; Youn, H.; Her, J.; Kim, S. K.; Lee, J.; Shin, J. H.; Ban, C. Electrochemical aptasensor of cardiac troponin I for the early diagnosis of acute myocardial infarction. *Anal. Chem.* **2015**, *87*, 9869.

(31) Saenger, A. K.; Rodriguez-Fraga, O.; Ler, R.; Ordonez-Llanos, J.; Jaffe, A. S.; Goetze, J. P.; Apple, F. S. Specificity of B-type natriuretic peptide assays: cross-reactivity with different BNP, NT-proBNP, and propBNP peptides. *Clin. Chem.* **2017**, *63*, 351–358.

(32) Pfister, R.; Scholz, M.; Wielckens, K.; Erdmann, E.; Schneider, C. A. Use of NT-proBNP in routine testing and comparison to BNP. *Eur. J. Heart Failure* **2004**, *6*, 289–293.

(33) Seferian, K. R.; Tamm, N. N.; Semenov, A. G.; Mukharyamova, K. S.; Tolstaya, A. A.; Koshina, E. V.; Kara, A. N.; Kraznoselsky, M. I.; Apple, F. S.; Esakova, T. V.; Filatov, V.; Katrukha, A. G. The brain natriuretic peptide (BNP) precursor is the major immunoreactive form of BNP in patients with heart failure. *Clin. Chem.* **2007**, *53*, 866–873.